

A high frequency chaotic signal generator: A demonstration experiment

Prodyot Kumar Roy^{a)}

Department of Physics, Presidency College, Calcutta 700 073, India

Arijit Basuray^{b)}

Research Division, Neo Tele-Tronix Pvt. Ltd., 6/7 Bijoygarh, Calcutta 700 032, India

(Received 24 August 2001; accepted 24 June 2002)

We discuss a simple oscillator that is capable of producing chaotic as well as periodic signals. The circuit design is straightforward and can easily be implemented in a standard undergraduate physics laboratory. The signal generator is suitable for demonstrating how the nonlinearity of the circuit elements can affect the output of an electronic device. © 2003 American Association of Physics Teachers. [DOI: 10.1119/1.1515481]

I. INTRODUCTION

Within the past few decades, scientists, mathematicians, and engineers have realized that a large variety of physical systems exhibit very complicated dynamical behavior. This complicated behavior, popularly called chaos, occurs so frequently that examples of simple nonlinear dynamics are finding their way into the undergraduate curriculum.¹

In this paper we focus on chaotic oscillators. The development of such oscillators and their synchronization is an active field of research in communications technology.² High frequency chaotic oscillators have immense potential for applications in secure communication because chaotic oscillators such as the universal circuit designed by Chua³ or the electronic analog of the Lorenz system⁴ are low frequency devices and are not suitable as communication devices.

The present design is a modified version of the Colpitts oscillator described in standard textbooks.⁵ It is simple enough, yet all the major features of chaos can be understood analytically. The design can be integrated easily into an undergraduate physics laboratory. One of the advantages of the Colpitts oscillator is that its frequency can vary from a few hertz to a few giga hertz (microwave region), depending on the circuit components chosen. Another advantage is that the active device possesses an intrinsic nonlinearity (the current-voltage relation is exponential), which can easily give rise to regular (periodic) oscillations or chaotic behavior depending upon the choice of parameters. In Sec. II we describe the circuit design of the signal generator. In Sec. III we briefly outline the theoretical analysis of the dynamical system. A few diagrams show the richness of the attractor. Section IV deals with the implementation of the circuit in the laboratory. Here we give our experimental results as well as the simulated results obtained using PSPICE. Finally, in Sec. V we discuss various possibilities for future work.

II. ANALOG CIRCUIT

A common-base transistor configuration is used as shown in Fig. 1. The resistor R and inductor L are connected in series between the collector and positive supply voltage. Another resistor R_1 is connected between the emitter and the negative supply. Such a connection is rather unconventional. Care must be taken to choose a value of R_1 that is not too low because a high current through the transistor will damage it. The capacitors C_1 and C_2 are used to adjust the oscillator frequency of the circuit, which depends as usual on the combination of C_1 , C_2 , and the inductor L . The probes

of the cathode ray oscilloscope (not shown in Fig. 1) are connected so that the collector and the emitter voltages are measured with respect to the ground.

III. ANALYSIS OF THE DYNAMICAL SYSTEM

The schematic diagram is given in Fig. 1. By applying Kirchhoff's laws, we find that the current and voltage equations are

$$C_1 \frac{dV_{C_1}}{dt} = I_L - I_C, \quad (1)$$

$$C_2 \frac{dV_{C_2}}{dt} = I_L - I_C + I_E - I_R, \quad (2)$$

and

$$V_{CC} = V_{C_1} + V_{C_2} + L \frac{dI_L}{dt} + I_L R, \quad (3)$$

where V_{C_1} and V_{C_2} are the voltages across the capacitors and I_L is the current through the inductor.

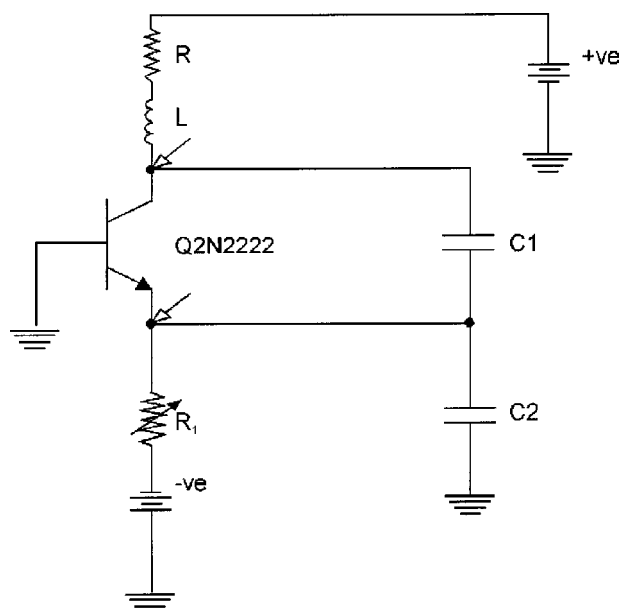


Fig. 1. Schematic diagram of the circuit.

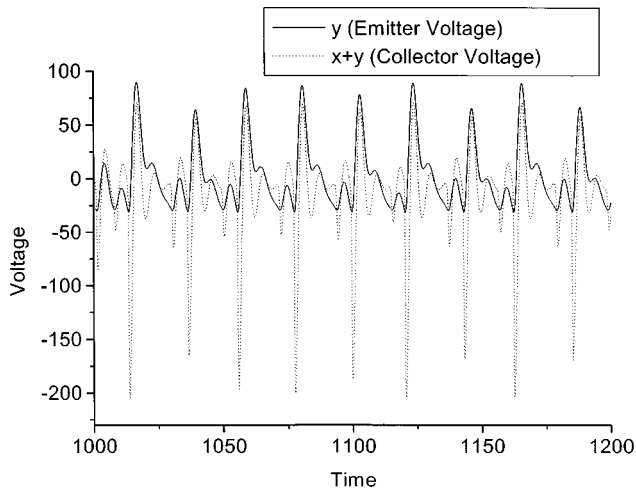


Fig. 2. Evolution [from numerical solutions of Eqs. (4)–(6)] of the (scaled) emitter and collector voltages for $R_1=270 \Omega$.

We replace the collector current I_C by αI_E , and remember that the emitter current I_E is exponential, namely, $I_E = I_S[\exp(V_{BE}/V_T) - 1]$. I_S is the reverse saturation current, V_{BE} is the base emitter voltage, and V_T is given by V_T

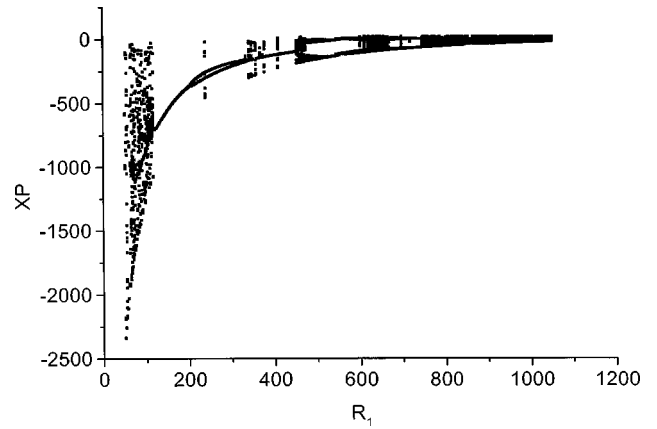


Fig. 4. Bifurcation diagram obtained by plotting XP, the x -coordinate of the penetrating points on the Poincaré surface, at various values of R_1 .

$=kT/e$. (T denotes the absolute temperature, k the Boltzmann constant, and e the electronic charge.) In our case, $V_{BE} = -V_{C2}$.

It is general practice to write the equations in dimensionless form. To do so we scale voltages by V_T and time by $1/\omega_0$, where ω_0 is the natural frequency of oscillation of the LC tank circuit, that is, $\omega_0 = 1/\sqrt{LC}$. Thus we have

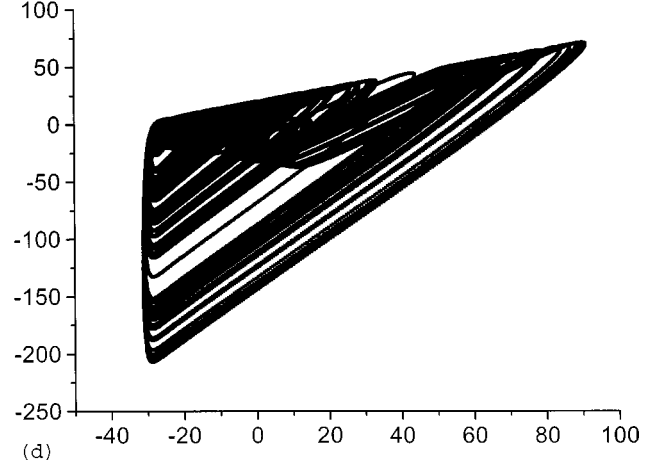
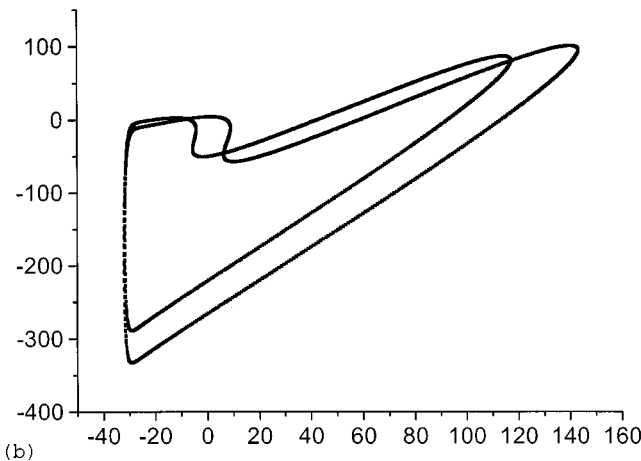
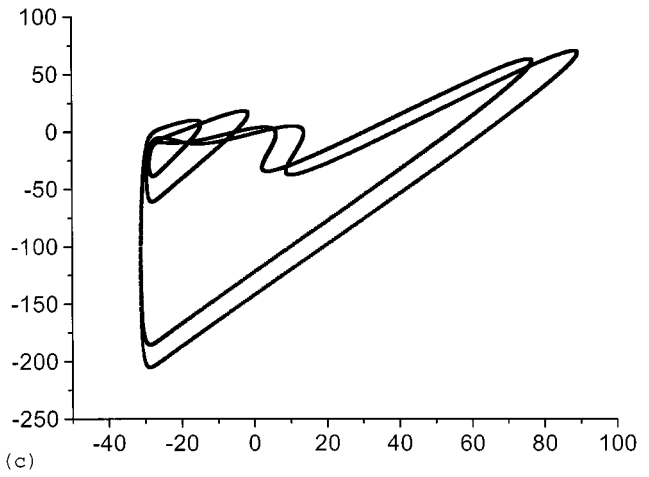
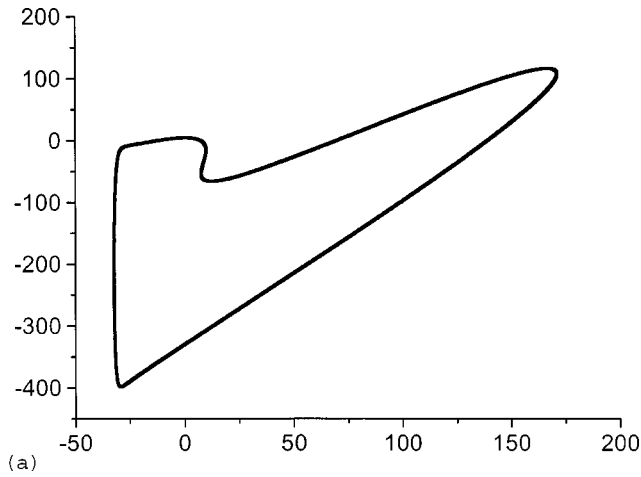


Fig. 3. Phase portraits of the chaotic attractor. The emitter voltage y vs $x+y$ (collector voltage). (a) $R_1=202 \Omega$, (b) $R_1=240 \Omega$, (c) $R_1=463 \Omega$, (d) $R_1=470 \Omega$.

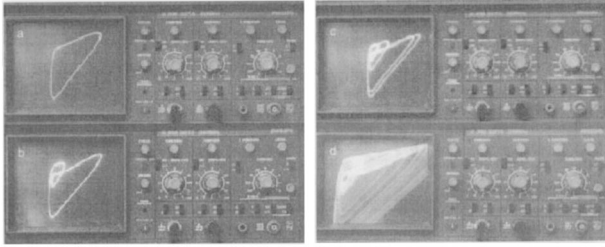


Fig. 5. Phase portrait as observed on an oscilloscope display. The emitter voltage is in the X mode and the collector voltage is in the Y mode. (a) $R_1 = 160 \Omega$, (b) $R_1 = 188 \Omega$, (c) $R_1 = 211 \Omega$, (d) $R_1 = 242 \Omega$.

$$\frac{dx}{d\tau} = Q\kappa[z - \alpha\gamma(e^{-y} - 1)], \quad (4)$$

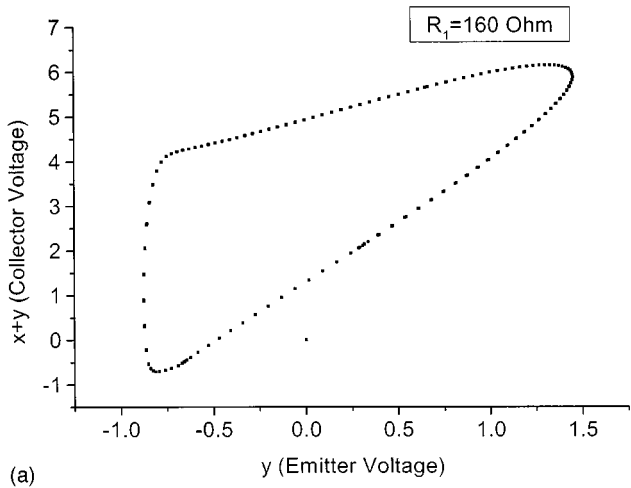
$$\frac{dy}{d\tau} = Q(1 - \kappa)\left[z + (1 - \alpha)\gamma(e^{-y} - 1) - \rho\left(y + \frac{5}{V_T}\right)\right], \quad (5)$$

$$\frac{dz}{d\tau} = -\frac{x + y + z}{Q}, \quad (6)$$

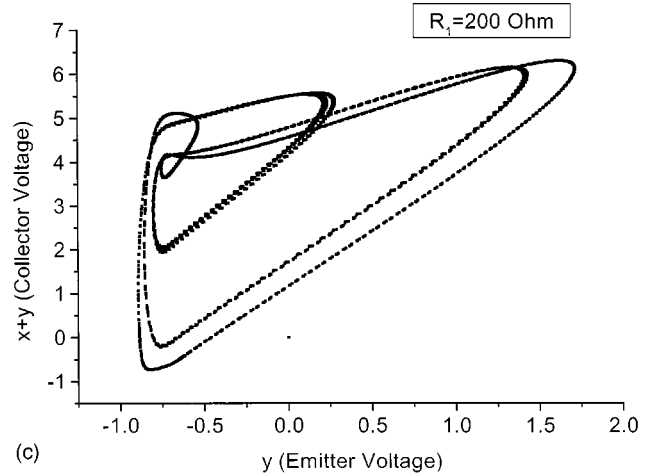
where $x = V_{C1}/V_T$, $y = V_{C2}/V_T$, $z = RI_L/V_T$, and $\tau = \omega_0 t$. Q is the quality factor, that is, $Q = \omega_0 L/R$. We also have $\kappa = C2/(C1 + C2)$, while $\gamma = I_S R/V_T$ is a ratio of two voltages, and $\rho = R/R_1$.

The numerical simulation of Eqs. (4)–(6) was done using a fourth order Runge–Kutta algorithm. For the simulation we used the following values of the circuit components: $L = 91 \mu\text{H}$, $R = 33 \Omega$, and $C1 = C2 = 0.068 \mu\text{F}$. The variable resistor R_1 ranges from 50 to 1000 Ω . The reverse saturation current I_S for transistor Q2N2222 in Fig. 1 was taken to be $14.34 \times 10^{-15} \text{ A}$ (from the transistor manual) and $V_T = 0.027 \text{ eV}$. (The same values were chosen for the simulations using PSPICE in Sec. IV.) Figure 2 shows the evolution of the scaled voltages across the capacitors $C1$ and $C2$. The phase portrait in Fig. 3 shows the chaotic attractor where we have plotted the collector voltage $x + y$ versus the emitter voltage y (with respect to the ground).

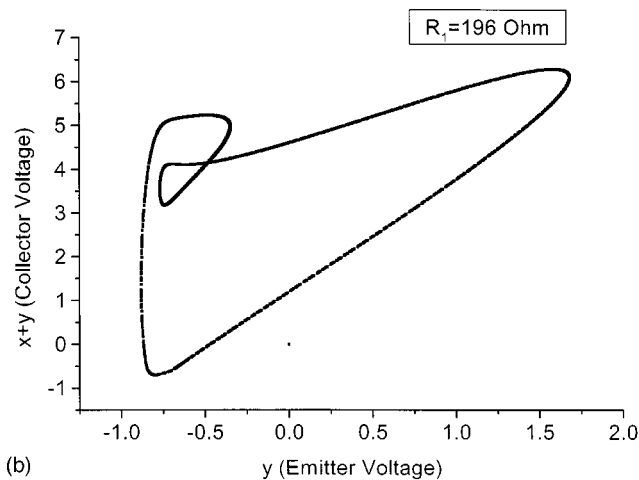
As mentioned, the oscillator can oscillate periodically if we suitably choose the circuit components. To understand how the oscillation changes with the variation of a parameter, we would normally look at the bifurcation diagram. One simple way of obtaining such a diagram is to plot the maxima of the time series against the value of this parameter.



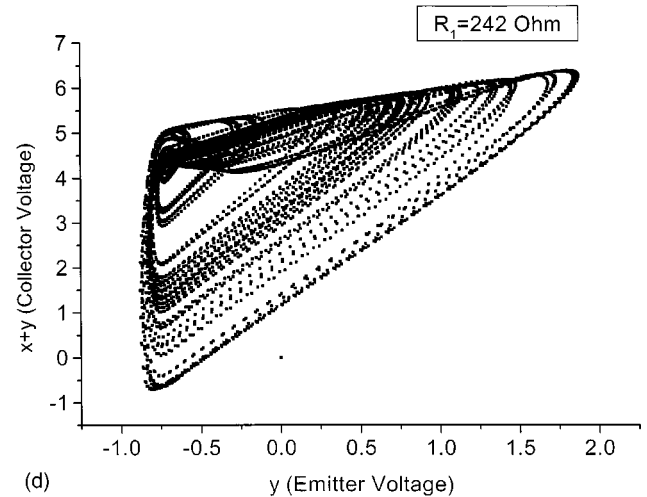
(a)



(c)



(b)



(d)

Fig. 6. Phase portrait as simulated by PSPICE. The emitter voltage is plotted along the X axis and the collector voltage is plotted along the Y axis. (a) $R_1 = 160 \Omega$, (b) $R_1 = 196 \Omega$, (c) $R_1 = 200 \Omega$, (d) $R_1 = 242 \Omega$.

Alternatively, we can plot the coordinates of the Poincaré surface plot. As the system evolves, it follows a path in phase space which is referred to as an orbit or trajectory. To extract information from the latter, it is often useful to reduce a continuous time system to a discrete time map by the Poincaré surface of section method, where a suitable surface of section (the dimension of which is always one less than that of the original phase space) is chosen and the intersections of the orbit with the surface is observed.

In our example we have chosen $y = -25$ as our Poincaré surface of section and noted the coordinates (XP, ZP) of the penetration points. In Fig. 4 we plot XP vs R_1 to obtain the bifurcation diagram. It clearly shows the regions where the output signal becomes chaotic and the phenomenon of period doubling. The bifurcation diagrams in higher dimensions will not be discussed here, but are essential for a full bifurcation analysis.⁶

IV. EXPERIMENTAL RESULTS

We have used circuit components that are commercially available. The value of the inductance L as measured by a LCR (digital) bridge is $91 \mu\text{H}$ with resistance 0.7Ω . The value of the external resistance R is 33Ω . The capacitors C_1 and C_2 are 0.069 and $0.072 \mu\text{F}$, respectively. The variable resistor R_1 ranges from 47 to 1047Ω . All these values were measured by a digital multimeter. The measured values differ slightly from the values printed on the components. We have used the high gain transistor Q2N2222 in our circuit. The output as observed on an oscilloscope display are presented in Fig. 5. The emitter voltage and collector voltage were observed in the $X-Y$ mode of the oscilloscope as mentioned in Sec. II. The results obtained by numerical simulation using PSPICE are presented in Fig. 6.

V. DISCUSSION

The oscillator system is suitable for upper division students in a physics laboratory course. Students wanting to pursue an in-depth study can, for example, perform a detailed bifurcation analysis, but this analysis requires a strong mathematical background and good programming knowledge. The circuit components are easily available in any standard lab.

An alternative circuit⁷ exists that requires the design of a constant current generator with output of the order of I_S , which is a rather difficult task. In the present design⁸ we have avoided this need, and hence the circuit is less expensive and easier to implement.

One can also try to modify the model equations used in Sec. III. Although the theoretical model predicts chaos at low

values of R_1 (see the bifurcation diagram in Fig. 4), the PSPICE simulation does not give such results. There are various reasons for this discrepancy. For example, the experiment has been performed at room temperature (around 35°C), but the PSPICE results are standardized at 27°C . Moreover, the circuit components in PSPICE are assumed to be perfect. The simple exponential characteristic of the transistor assumed for simulations may be improved to obtain a more realistic result. Investigations along this line would be an interesting project in mathematical modeling.

We can apply a sinusoidal signal to the base of the transistor to understand the dynamics of a driven oscillator. The observation on an oscilloscope display of the formation of a torus and its breakdown is quite interesting.

We have presented the results of our measurements using a dual trace high frequency oscilloscope. Alternatively, data collection and analysis can be done using software packages such as LABVIEW. The fixed point solution, stability, existence of limit cycles, etc., can be done using MATHEMATICA, MATHCAD, etc. Interested readers may request source code (in QUICK BASIC) from the authors.

ACKNOWLEDGMENTS

The authors warmly acknowledge useful discussions with Shyamal Kumar Dana and Bishyapriya Mukhopadhyay.

^aElectronic mail: pkpresi@yahoo.co.in

^bElectronic mail: ntpl@cal.vsnl.net.in

¹R. C. Hilborn and N. B. Tufillaro, "Resource Letter: ND-1: Nonlinear Dynamics," Am. J. Phys. **65** (9), 822–834 (1997).

²K. M. Cuomo, A. V. Oppenheim, and S. H. Isabelle, "Spread spectrum modulation and signal masking using synchronized chaotic systems," MIT Research Laboratory of Electronics, Tech. Rep. No. 570, 1992. Also see K. M. Cuomo and A. V. Oppenheim, "Synchronized chaotic circuits and systems for communications," MIT Research Laboratory of Electronics, Tech. Rep. No. 575, 1992). Both reports are available from <http://allegro.mit.edu/dspg/publications/TechRep/>.

³L. O. Chua, L. O. Wu, A. Hsong, and G. Q. Zhong, "A universal circuit for studying and generating chaos. I Route to chaos," IEEE Trans. Circuits Syst., I: Fundam. Theory Appl. **40** (10), 732–744 (1993).

⁴K. M. Cuomo and A. V. Oppenheim, "Circuit implementation of synchronized chaos with application to communications," Phys. Rev. Lett. **71**, 65–68 (1993).

⁵M. H. Rashid, *Microelectronic Circuits: Analysis and Design* (PWS, Boston, 1999); P. Horowitz and W. Hill, *The Art of Electronics* (Cambridge U.P., Cambridge, 1989).

⁶H. Kawakami and R. Lozi, *Structure and Bifurcation of Dynamical Systems* (World Scientific, Singapore, 1992).

⁷F. O'Caibre, G. M. Maggio, and M. P. Kennedy, "Devaney chaos in an approximate one-dimensional model of the Colpitts oscillator," Int. J. Bifurcation Chaos Appl. Sci. Eng. **7** (14), 2561–2568 (1997).

⁸M. P. Kennedy, "Chaos in the Colpitts oscillator," IEEE Trans. Circuits Syst., I: Fundam. Theory Appl. **41** (11), 771–774 (1994).